

## Supplementary Information for

# Correlating the scattered intensities of P3HT and PCBM to the current densities of polymer solar cells

*Enrique D. Gomez\**, *Katherine P. Barteau*, *He Wang*, *Michael F. Toney*, and *Yueh-Lin Loo\**

## **1. Methods**

### *1.1. Fabrication of devices and samples for X-ray scattering experiments*

Indium tin oxide (ITO) on glass (Colorado Concept Coatings, 120-160 nm thickness, 9-15  $\Omega$ /sq.) was used for this study. Substrates were modified by either depositing a molecular layer of 1H,1H,2H,2H-perfluorotetradecylphosphonic acid, FSAM (Specific Polymers), *n*-tetradecylphosphonic acid, HSAM, (Alfa Aesar) or 100 nm of poly(3,4-ethylenedioxythiophene) poly(styrenesulfonate), PEDOT:PSS, (Clevios P, H.C. Starck) on ITO. Deposition of HSAM or FSAM were carried out at ambient conditions by first dissolving the molecule at 0.2 mM concentration in anhydrous THF and then submerging the pre-cleaned ITO/glass substrates in the solution for 16 hrs. Afterwards, the substrates were rinsed extensively with THF and methanol. The substrates were then placed in an oven for 24 hrs at 130 °C before they were rinsed again with isopropanol or methanol. As-purchased PEDOT:PSS dispersions were spin coated onto ITO at 2000 rpm for 120 s. The PEDOT:PSS film, approximately 100 nm thick, was annealed at 170 °C for 20 min. All substrate processing was carried out at ambient conditions.

Deposition of the active layer on ITO and modified ITO substrates was carried out inside a nitrogen glove box (<1ppm O<sub>2</sub> and H<sub>2</sub>O) equipped with an integrated spin coater and thermal evaporator. P3HT (50 kg/mol M<sub>w</sub>, 96% H-T regioregular, Merck) and PCBM (Nano-C) were codissolved in chlorobenzene at a 1:0.8 P3HT to PCBM mass ratio and a total concentration of

24 mg/mL. The solution was annealed for 24 hrs at room temperature, and then heated to 90 °C for 10 s on a hot plate before it was spin coated at 500 rpm to form a uniform film of 150 nm. All thermal annealing took place inside the glove box on a digital hot plate equipped with an independent surface thermometer prior to top electrode deposition. Aluminum was evaporated at  $10^{-6}$  torr at 0.1-0.4 Å/s for the first 20 nm and 1 Å/s for the last 80 nm, for a total metal thickness of 100 nm. Samples for X-ray diffraction studies were prepared in an analogous fashion, but aluminum was not deposited on the photoactive layer surface.

### *1.2. Device testing*

After solar cell fabrication, devices were transferred into an attached glove box for testing without exposure to the atmosphere. A 300 W Xe solar simulator (Newport) was used with an AM1.5G filter and metallic fused-silica neutral density filters (Melles Griot) to match the solar spectrum at the standard 100 mW/cm<sup>2</sup> illumination intensity. *J-V* characteristics were obtained by making contact through indium-coated probes connected to a Keithley 2600 series source meter controlled through an in-house Labview program.

### *1.3. X-ray scattering experiments*

X-ray diffraction experiments took place on beamline 11-3 at the Stanford Synchrotron Radiation Laboratory. The X-ray wavelength was 0.975 1/Å. Rocking curves were obtained by rocking the sample (1.55 to 1.8°) during data acquisition. Grazing incidence diffraction experiments were carried out at an incident angle of 0.11°. Five sequential scans were performed for grazing-incidence experiments and were averaged together. The data were corrected for scattering from air, scattering from the substrate and for the polarization of incident X-rays (98%, in-plane). Scattering intensities were normalized by the incident photon flux and acquisition time.

#### 1.4. X-ray data analysis

For the rocking curves, X-rays scattered for a polar angles,  $\omega$ , of 60 - 90° ( $\omega = 0^\circ$  at the substrate normal) are blocked by the substrate. We have thus opted to stitch together our GIXD data with that acquired during rocking experiments to construct full pole figures of the P3HT (100) reflection. The stitching process is done by scaling the grazing-incidence data to match the rocking data near  $\omega = 55^\circ$ , where  $\omega$  is the polar angle (see Figure 1 of the main text)<sup>1</sup>. Rocking data is used for  $\omega < 55^\circ$ , while grazing-incident data is used for  $\omega > 55^\circ$ . The construction of these full pole figures enables quantitative comparison of the extent of crystallinity of P3HT across different samples. Figure 1d of the main text shows the full pole figures for the same P3HT/PCBM films on which the GIXD data in Figures 1a and b were acquired. The sharp downturn in the intensity near  $\omega = -90^\circ$  is an artifact of the experimental setup as the beam stop blocks any scattered intensities in this range. To compute the P3HT crystallinity, we integrate the product of the pole figure and  $\sin(\omega)$  over all  $\omega$ .  $\sin(\omega)$  is a necessary correction for the thin film geometry. Absolute quantification of the extent of crystallinity of P3HT is notoriously difficult and would require, for example, experimentation with a sample of known crystallinity.

We compute the PCBM scattered intensity by first normalizing the GIXD intensity of the PCBM reflection at 1.4 1/Å against that of the P3HT (100) reflection acquired during the same scan. This normalization allows us to account for differences in scattered intensities due to small changes in the incident angle during GIXD experiments and enables a meaningful comparison across all samples. It follows that this ratio is directly proportional to the structuring of PCBM after it is normalized against the crystallinity of P3HT, as extracted from the full pole figure analysis outlined above:

$$I_{\text{PCBM,corrected}} / I_{\text{P3HT,crystallinity}} = I_{\text{PCBM,GIXD}} / I_{\text{P3HT,GIXD}} \quad (\text{S1})$$

here  $I_{\text{PCBM,corrected}}$  is a quantity that is directly proportional to the PCBM scattered intensity;  $I_{\text{P3HT,crystallinity}}$  is the extracted intensity from the full pole figure analysis of the P3HT (100) reflection and is therefore proportional to the crystallinity of P3HT;  $I_{\text{PCBM,GIXD}}$  and  $I_{\text{P3HT,GIXD}}$  represent the integrated intensities of the PCBM and P3HT reflections from GIXD data, respectively. Due to the experimental geometry, the GIXD data does not include scattering from crystals oriented within  $\sim 2$  degrees of the surface normal. In calculating  $I_{\text{P3HT,GIXD}}$ , we correct for this effect using the rocking curve data near  $\omega \sim 0^\circ$ . Furthermore, equation 1 assumes that the orientation of P3HT does not change significantly between samples, an assumption that is valid given that we do not observe large changes in the P3HT(100) pole figures across our samples. The integrated intensity of the PCBM reflections is obtained through deconvolution of the PCBM peaks as described in Section 3 below. Applying equation S1 to the extracted intensities of the GIXD traces thus allows quantitative comparisons of the PCBM scattered intensity among all samples. We take the measured PCBM scattered intensity to be directly related to the amount of PCBM in PCBM/P3HT films which adopts the same local structure of PCBM-only films. Thus, we hypothesize that the changes in our scattered intensity are due to changes in the aggregation characteristics of PCBM in the active layers.

## **2. Grazing-incidence X-ray diffraction (GIXD) images of PCBM films**

Figure S1 shows 2D GIXD images of PCBM films (15 mg/mL, chlorobenzene) deposited via spin coating on ITO (Figures S1a and S1c) and on PEDOT:PSS-coated ITO substrates (Figures S1b and S1d). Data taken on unannealed films are shown in Figures S1a and S1b, while data on films annealed for 30 min at 165 °C are shown in Figures S1c and S1d. We were unable

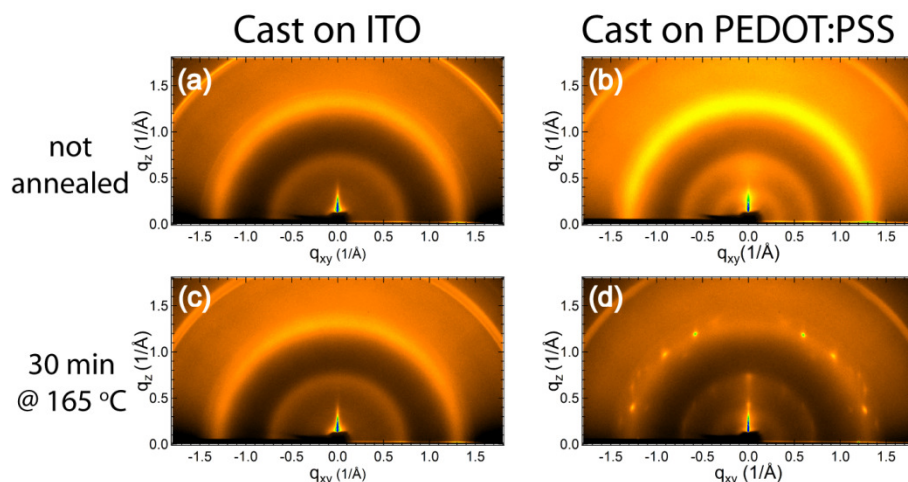


**Figure S1.** Two-dimensional grazing-incidence X-ray diffraction images of PCBM films (a), (b) not thermally annealed and (c), (d) annealed for 30 min @ 165 °C. Images were obtained from films cast on ITO (Figures S1a and S1c) and PEDOT:PSS (Figures S1b and S1d). Note the highly crystalline structure evident from the large number of spots in Figure S1d.

to spin coat PCBM on HSAM- or FSAM-modified ITO substrates, most likely due to the low surface energy of these substrates. The GIXD images in Figures S1a through S1c exhibit a reflection that is characteristic of PCBM at 1.4 1/Å; the intensity of this reflection appears to be uniform azimuthally. The GIXD image in Figure S1d, on the other hand, appears to be different from the other GIXD images. Specifically, the GIXD image in Figure S1d shows a large number of spots, showing that annealing PCBM on PEDOT:PSS leads to crystallization of the PCBM with preferentially oriented crystals. Although we have no concrete explanation for this phenomenon at this time, we hypothesize that a combination of surface energetics and surface roughness can play a role in promoting the crystallization of PCBM.

### **3. Deconvolution of PCBM and P3HT reflections**

In order to deconvolute the constituent P3HT and PCBM peaks in P3HT/PCBM GIXD data, we first analyze data from PCBM- and P3HT-only films. Figure S2a shows the azimuthally-averaged intensity as function of  $q$  for a well-ordered PCBM film (Figure S1d). The data can be deconvoluted into four Lorentzians: three individual peaks corresponding to

crystalline PCBM reflections at  $1.25 \text{ 1/\AA}$ ,  $1.38 \text{ 1/\AA}$  and  $1.46 \text{ 1/\AA}$ , and a fourth broad peak at  $1.31 \text{ 1/\AA}$ , most likely corresponding to an amorphous phase. Assignment of the crystalline PCBM peaks is beyond the scope of this paper. A similar deconvolution procedure can be performed for P3HT-only films, as shown in Figure S2b.

Using the peak positions and the peak width of the amorphous peaks obtained in Figure S2 for both P3HT and PCBM, we can now deconvolute the individual contributions to the scattered intensity for data generated from P3HT/PCBM films. Figure S3 shows azimuthally-averaged GIXD data for P3HT/PCBM films and the resulting constituent peaks. The PCBM scattered intensity is computed as the sum of the area of all the constituent PCBM peaks. The aggregation of PCBM in P3HT/PCBM mixtures prior to PCBM crystallization contributes to an increase of the PCBM scattered intensity through an increase in the average number of adjacent PCBM molecules or increase in the extent of local organization. Thus, we take the PCBM scattered intensity as a measure of the extent of aggregation and order of PCBM, even when distinct crystalline reflections are not present.

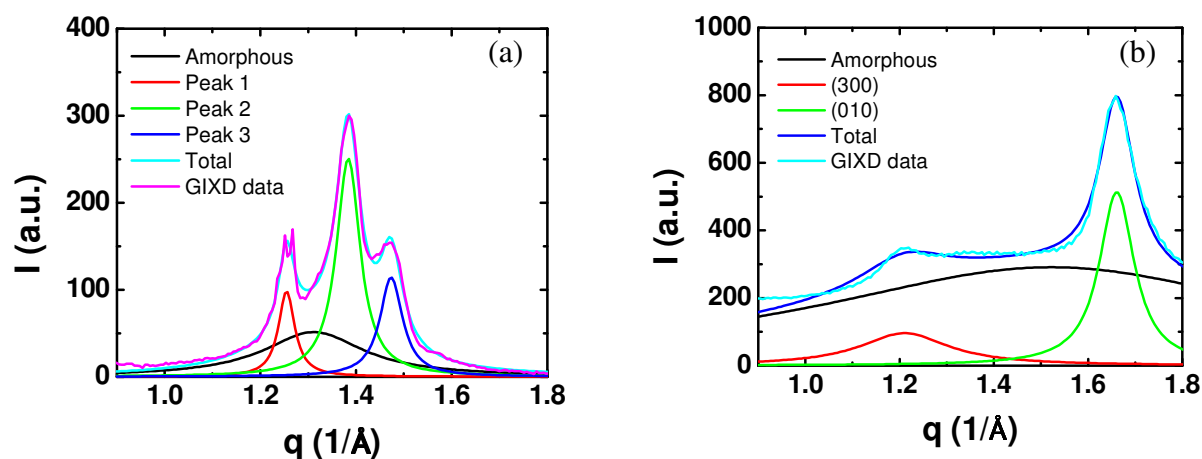


**Figure S2.** (a) GIXD intensity (pink), constituent peaks and sum of peaks (light blue, Total) for a PCBM-only film. (b) GIXD intensity (light blue), constituent peaks and sum of peaks (blue, Total) for a P3HT-only film.

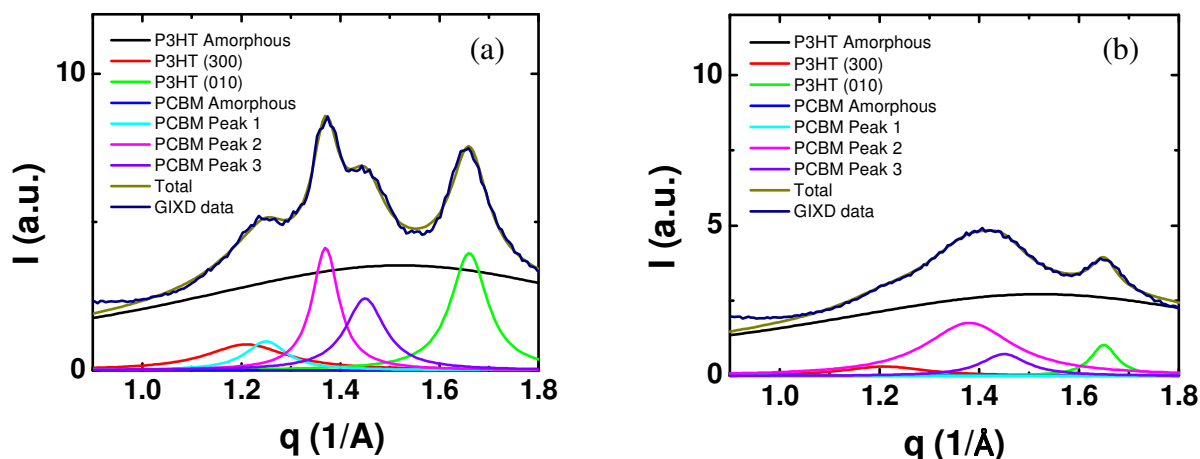


**Figure S3.** GIXD intensity (dark blue), constituent peaks and sum of peaks (gold, total) for P3HT/PCBM films (a) annealed for 240 min at 130 °C and (b) not annealed.

Alternatively, we can compute the PCBM scattered intensity by integrating between  $1.22 \leq q \leq 1.54 \text{ 1/Å}$  and applying equation 1 of the main text with a linear background subtraction between 1.21 and  $1.55 \text{ 1/Å}$ . As shown in Figure S4, the results are similar to extraction of PCBM scattered intensities through deconvolution (compare with Figure 3 of the main text). In both methodologies for quantifying the PCBM scattered intensity, our experimental geometry does not include contributions from crystals oriented within  $\sim 6^\circ$  of the surface normal. Given that PCBM is always isotropic in our P3HT/PCBM samples, we do not expect this experimental limitation to affect our results.

#### **4. Extent of out-of-plane $\pi$ -stacking from rocking curve intensities near $\omega = 90^\circ$**

Figure S5 shows X-ray rocking curves for P3HT/PCBM films as a function of polar angle  $\omega$ . As shown in Figure 4 of the main text, we estimate the extent of out-of-plane P3HT  $\pi$ -stacking in P3HT/PCBM films by integrating the rocking curve intensity between  $\omega = 75^\circ - 80^\circ$ . We chose to use  $75^\circ - 80^\circ$  to avoid the intensity enhancement near  $\omega = 90^\circ$  due to the scattering geometry in Figure S5. As shown in Figure S6, the rocking curve intensity integrated between  $\omega$

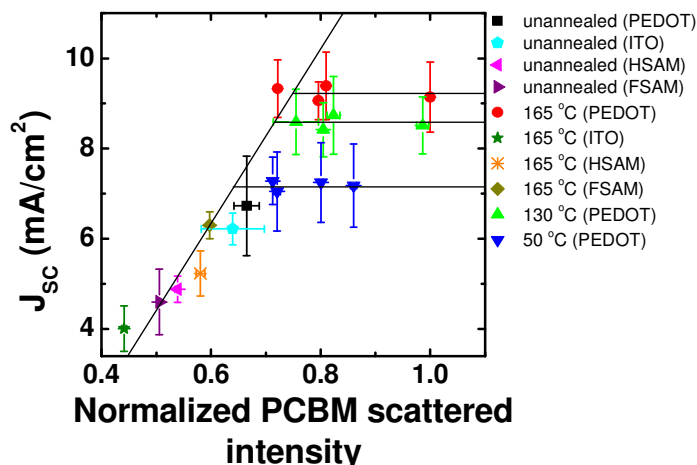


**Figure S4.**  $J_{SC}$  vs normalized PCBM scattered intensity where the scattered intensity is computed using a linear background subtraction and eqn 1 of the main text. The PCBM scattered intensity is normalized to the largest PCBM scattered intensity.

$= 80^\circ - 90^\circ$  is quantitatively the same as the intensity integrated between  $75^\circ - 80^\circ$ , confirming that our results are the same with either choice of integration range.

In estimating the extent of out-of-plane P3HT  $\pi$ -stacking from rocking curves we ignore contributions to the rocking curve intensity near  $\omega = 90^\circ$  from P3HT crystals oriented with both the (100) and (010) planes parallel to the substrate normal. We expect the population of these

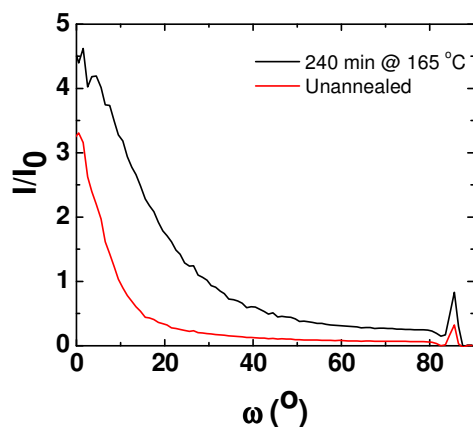


**Figure S5.** Rocking curves of the P3HT/PCBM films as a function of the polar angle,  $\omega$ . A linear background was calculated using scattered intensities away from the Bragg reflections ( $q \sim 0.3$  and  $0.46$   $1/\text{\AA}$ ) and subtracted from the data. For the data shown in Figure 4 of the main text, we integrate the rocking curve intensity between  $\omega = 75^\circ$  and  $80^\circ$ .

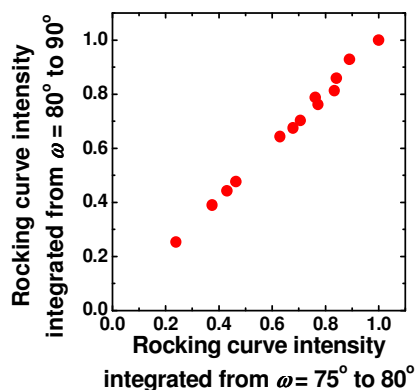


**Figure S6.** Rocking curve intensity integrated from  $\omega = 80^\circ$  to  $90^\circ$  as a function of the rocking curve intensity integrated from  $\omega = 75^\circ$  to  $80^\circ$ . Both intensities are normalized to the largest intensity found in our samples.

crystal orientations to be negligibly small because P3HT generally does not orient with its chain axis perpendicular to the substrate.<sup>2-4</sup>

### **5. Alternative methodology for quantifying the extent of out-of-plane $\pi$ -stacking**

As an alternative to quantifying the extent of out-of-plane  $\pi$ -stacking from rocking curves at  $\omega \sim 90^\circ$ , we can use the P3HT (010) reflection in the  $q_z$  direction from our GIXD images. We again turn to equation 1 to estimate the extent of out-of-plane P3HT  $\pi$ -stacking,  $I_{P3HT(010),corrected}$ , by integrating the (010) intensity ( $1.58 \leq q_z \leq 1.78 \text{ 1/\AA}$ ) in the  $z$ -direction over  $0.05 \text{ 1/\AA}$  ( $q_{xy}$ ) after subtracting a linear contribution we attribute to an isotropic background. Note that  $I_{PCBM,corrected}$  is replaced by  $I_{P3HT(010),corrected}$  and  $I_{PCBM,GIXD}$  is replaced by  $I_{P3HT(010),GIXD}$  in equation 1. Due to the grazing-incidence geometry, however, the scattering vector is tilted by  $\sim 7^\circ$  with respect to the substrate normal. Crystals with their (010) planes tilted less than  $7^\circ$  thus do not contribute to the GIXD out-of-plane (010) intensity. Nevertheless, our results, shown in Figure S7, indicate a linear correlation between the device  $J_{SC}$  and the out-of-plane P3HT (010) intensity. The intensity is normalized to the largest value found in our samples. This is consistent with the observed trend of Figure 4 of the main text, confirming that the structure-

function correlations reported herein are real, and not artifacts of data processing. Despite the large error bars, both Figure S7 and Figure 4 implicate a non-negligible correlation between the device  $J_{SC}$  and the out-of-plane P3HT  $\pi$ -stacking.

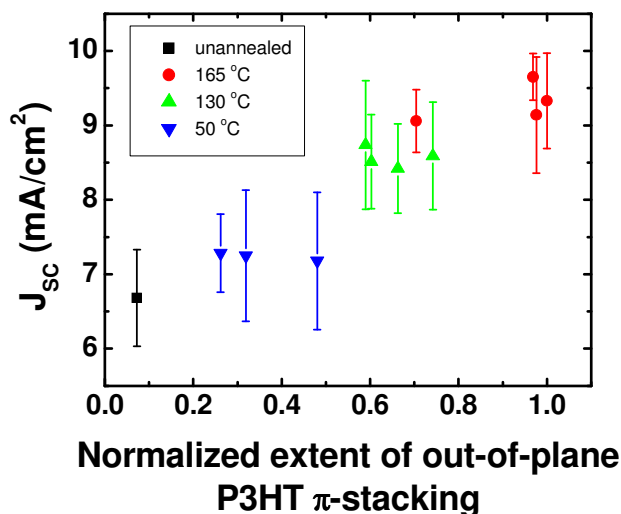


**Figure S7.** Device  $J_{SC}$  vs normalized out-of-plane P3HT (010) intensity obtained from GIXD images and equation 1 of the main text of P3HT/PCBM films annealed at various temperatures. The out-of-plane intensity is normalized by the largest intensity in our samples. The samples included in this figure have PCBM scattered intensity > 0.6.

## **6. P3HT and PCBM scattered intensities obtained from X-ray scattering experiments**

In this study, we varied the annealing time and temperature of the active layer of P3HT/PCBM solar cells. Using rocking scans, GIXD data and eqn S1 we determined the P3HT crystallinity and PCBM scattered intensity. A summary of our results can be found in Table S1. Note that all values are normalized to the highest value measured in our samples.

**Table S1. Summary of the normalized\* P3HT crystallinity and PCBM scattered intensity obtained for all of the samples in this study.**

Anode	Annealing temperature (°C)	Annealing time (min)	P3HT crystallinity	PCBM intensity	(100) P3HT intensity ( $\omega = 90^\circ$ )
PEDOT:PSS	25	0	0.33	0.68	0.25
		5	0.36	0.64	0.39
	130	10	0.45	0.71	0.48
		30	0.35	0.58	0.44
		240	0.72	0.89	0.64
		5	0.85	1.0	0.76
		10	0.89	0.76	0.81
		30	0.79	0.88	0.70
	165	240	1.0	0.72 <sup>‡</sup>	0.67
		5	0.87	0.98	1.0
		10	0.51	0.79	0.79
		30	0.70	0.78	0.86
ITO	165	240	0.98	0.69 <sup>‡</sup>	0.93
		0	0.36	0.58	0.14
		30	0.72	0.44	0.43
		30	0.64	0.56	0.29
FSAM/ITO	25	0	0.31	0.50	0.19
	165	30	0.64	0.56	0.29
HSAM/ITO	25	0	0.31	0.46	0.15
	165	30	0.71	0.50	0.22

\*All samples are normalized to the largest value obtained in our study

<sup>‡</sup>These samples show clear evidence of PCBM crystallization

## 7. References

1. J. L. Baker, L. H. Jimison, S. Mannsfeld, S. Volkman, S. Yin, V. Subramanian, A. Salleo, A. P. Alivisatos and M. F. Toney, *Langmuir*, 2010, **26**, 9146-9151.
2. C. H. Woo, B. C. Thompson, B. J. Kim, M. F. Toney and M. J. Frechet, *Journal of the American Chemical Society*, 2008, **130**, 16324-16329.
3. C. W. Chu, H. C. Yang, W. J. Hou, J. S. Huang, G. Li and Y. Yang, *Applied Physics Letters*, 2008, **92**, 103306.
4. H. C. Yang, T. J. Shin, L. Yang, K. Cho, C. Y. Ryu and Z. N. Bao, *Advanced Functional Materials*, 2005, **15**, 671-676.